Medicinal Chemistry Research (2019) 28:591–607
https://doi.org/10.1007/s00044-019-02322-8

MEDICINAL CHEMISTRY RESEARCH

ORIGINAL RESEARCH

Xenicanes attenuate pro-inflammatory 5-lipoxygenase: Prospective natural anti-inflammatory leads from intertidal brown seaweed *Padina tetrastromatica*

Tima Antony[1,2] · Kajal Chakraborty[1]

Received: 16 September 2018 / Accepted: 22 February 2019 / Published online: 11 March 2019

Abstract

Two previously unreported xenicane class of novaxenicin-type xenicin diterpenoids (**1**–**2**) bearing cyclonona[*d*]furo [2,3-*b*] pyrandiol and three xeniolide-type diterpenoids with unprecedented octahydrocyclonona[*c*]pyran-3(1*H*)-one backbones (**3**–**5**) were separated from the organic extract of the intertidal seaweed *Padina tetrastomatica* (family Dictyotaceae), collected from southern India. The compounds were deduced to bear a xenicane moiety with a 2-oxabicyclo[7.4.0]tridecane cyclic system. The structures of these specialized metabolites were attributed based on the extensive nuclear magnetic resonance spectral analyses, and comparison of related compounds. Xeniolide-type diterpenes (**3–5**) registered significantly greater attenuation potential against pro-inflammatory 5-lipoxygenase (IC_{50} ~ 2.04 mM) than that exhibited by non-steroidal anti-inflammatory drug ibuprofen (IC_{50} 4.50 mM, $P < 0.05$). The xeniolide derivative octahydro-1,7-dihydroxy-4-(4^1-hydroxy-4^2-methylpropyl)-6-(6^1-hydroxy-6^2-propenyl)-10-methyl-cyclonona[*c*]pyran-3(1*H*)-one (**5**) exhibited comparable antioxidant activity (DPPH IC_{50} 1.73 mM) along with standard antioxidative agent α-tocopherol ($IC_{50} < 2$ mM). In silico molecular modelling studies were performed to designate the 5-lipoxygenase inhibitory mechanism of the xenicanes, and the comparison of docking parameters suggested that the xeniolide derivative **5** exhibited least binding energy of −11.56 kcal mol^{-1}, and that was corroborated with its greater inhibition potential against the pro-inflammatory enzyme. These results demonstrated that the xeniolide-type diterpenoids with previously unreported δ-lactone cyclononane framework might constitute promising anti-inflammatory leads with pro-inflammatory 5-lipoxygenase enzyme inhibitory activities.

Keywords *Padina tetrastromatica* · Xenicane-type diterpenoids · Xenicins · Xeniolides · Anti-inflammatory · 5-Lipoxygenase enzyme inhibitory

Introduction

Seaweeds were viewed as promising sources of bioactive metabolites with functional food properties and pharmacological potentials (Plaza et al. 2008; Lann et al. 2016). Natural antioxidants in seaweeds were recognized to deter pathophysiological conditions leading to oxidative stress conditions and increase the shelf life of food ingredients (Jimenez-Escrig et al. 2001). Among various seaweeds, those belonging to the class Phaeophyceae (brown seaweed) were found to be potential sources of antioxidants and bioactive pharmacophores (Kang et al. 2011; Kindleysides et al. 2012). The brown seaweeds belonging to the family Dictyotaceae were considered as one of the potential sources of biologically active diterpenoid metabolites (Blunt et al. 2009), and among which xenicanes were recognized to be an interesting class of bioactive leads, which were

These authors contributed equally: Tima Antony, Kajal Chakraborty

Supplementary information The online version of this article (https://doi.org/10.1007/s00044-019-02322-8) contains supplementary material, which is available to authorized users.

✉ Kajal Chakraborty
kajal_cmfri@yahoo.com
kajal.chakraborty@icar.gov.in

[1] Marine Bioprospecting Section of Marine Biotechnology Division, Central Marine Fisheries Research Institute, Ernakulam North, P. B. No 1603 Cochin, India

[2] Department of Chemistry, Mangalore University, Mangalagangothri 574199 Karnataka State, India

isolated as one of the largest class of diterpenoids in marine organisms, with potential bioactive properties (Faulkner 1998; Viano et al. 2009).

Earlier reports of literature revealed the isolation of xenicane natural products from brown seaweeds *Dilophus fasciola*, *Dilophus spiralis* (Ioannou et al. 2009), *Dictyota* sp. (Viano et al. 2009), and *Padina pavonia* (Awad et al. 2008). Xenicane from the soft coral *Xenia elongata* was the first member of xenicane diterpenoids, and there were reports on further discovery of various bioactive xenia metabolites from the brown seaweeds. The bicyclic framework of xenicanes containing *trans*-fused system of ring A and cyclononane carbocyclic ring B possessing a nine-membered ring were reported from the soft coral, *Xenia elongata* (Vanderah et al. 1977). This unique family of xenia diterpenoids was classified into three main subclasses; xenicanes or xenicins, xeniolides and xeniaphyllanes with bicycle [7.2.0] undecane ring (Groweiss et al. 1983) along with recently reported azamilide with nine-membered monocarbocyclic framework acylated with $C_{16\text{-}20}$ fatty acids and an opened A ring. There were 53 main reports on xenia isoprenoids with several modifications in the ring and prenyl side chain (Blunt et al. 2009).

Seaweeds were recognized as invaluable marine resources in the Asian continent for use in food and pharmaceuticals (Barrento et al. 2016; Makkar and Chakraborty 2018ab). The brown seaweed *Padina sp*. was found to constitute a foremost share in the family Dictyotaceae and about 50 taxa of this genus were reported in various parts of the globe. Among them, *Padina tetrastromatica* (Hauck) (family Dictyotaceae) has been predominant in the Indo-Pacific region (Guiry and Nic-dhonncha 2003), and there were preliminary reports of their bioactive potentials (Chia et al. 2015; Mohsin et al. 2014). In the search for bioactive diterpenoids from this brown seaweed species, this work described the purification and characterizations of previously undescribed five xenicane classes of novaxenicin-type diterpenoids (**1**–**2**) bearing cyclonona[*d*]furo[2,3-*b*] pyrandiol and three xeniolide-type diterpenes with octahydrocyclonona[*c*]pyran-3(1*H*)-one backbones (**3**–**5**) from the organic EtOAc/MeOH (ethyl acetate-methanol) extract of the studied seaweed (Fig. 1) collected from the Gulf-of-Mannar of Peninsular India. The anti-inflammatory and antioxidant potential of the studied compounds were analysed by different in vitro assays, and various physicochemical descriptors were utilized to substantiate the structure–activity correlations of the studied diterpenoids. In silico molecular modelling studies were performed to designate the 5-lipoxygenase inhibitory mechanism of the studied xenicane analogues.

Materials and methods

General experimental procedures

A nuclear magnetic resonance (NMR) spectrometer {Bruker Avance DPX 500 (500 MHz), Rheinstetten, Germany} was used to obtain ^{1}H (500 MHz), ^{13}C (125 MHz) and other two-dimensional (2D)-NMR spectroscopic data, such as proton homonuclear correlation spectroscopy (^{1}H-^{1}H-COSY), C–H heteronuclear single-quantum correlation (HSQC), long-distance heteronuclear multiple bond correlation (HMBC), and nuclear overhauser effect spectroscopy (NOESY) by standard pulse sequences. Solvent deuterated chloroform $CDCl_3$ was taken as an aprotic solvent and tetramethylsilane (TMS) as a reference standard ($\delta 0$). NMR spectra were obtained by the software Bruker Top Spin™ 2. The documentation of Fourier-transform infrared (FTIR) spectra was carried out using potassium bromide (KBr) pellets on Perkin-Elmer Series 2000, FTIR spectrophotometer (scanning range of 4000 and 400 cm^{-1}). The UV data were acquired spectrometrically by using Varian Cary 50-UV-VIS spectrometer (Varian Cary, Walnut Creek, USA). The organic extracts and column fractions were concentrated to dryness using a rotary evaporator (Heidolph Instruments GmbH and Co., Schwabach, Germany) under reduced pressure. A flash chromatography instrument (Biotage AB SP1-B1A, Uppsala, Sweden) was used to fractionate the semi-purified fractions. Optical rotations were measured on an ATAGO AP-300 polarimeter. Reverse-phase high-pressure liquid chromatography (RP-HPLC) data were obtained by using Shimadzu LC-20AD pump device (Shimadzu Corporation, Nakagyo-ku, Japan), fitted with a C_{18} reverse-phase column (Luna 25 × 4.6 mm, 5 mm) (Phenomenex, Torrance, USA). Analytical high-pressure liquid chromatograph (HPLC) instrument (Shimadzu Corporation, Nakagyo-ku, Japan) connected to reverse-phase (RP)-C_8 and/or RP-C_{18} column(s) (bonded reverse-phase; Phenomenex, Torrance, USA; Luna 250 mm × 4.6 mm, 5 µm) fitted with a binary gradient pump (Shimadzu LC-20AD) column and photodiode array detector (SPD-M20A, Kyoto, Japan) was used to analyse the homogeneity of the studied compounds. Finer purification of the compounds were carried out with a semi-preparative RP-C_{18} HPLC column (Phenomenex, Torrance, USA; Luna 250 mm × 10 mm, 5 µm C_{18} 100A), fitted with a preparatory high-pressure liquid chromatograph (HPLC) instrument (Shimadzu Corporation, Nakagyo-ku, Japan). Gas-chromatographic mass-spectroscopic (GC-MS) analyses were acquired through electronic impact ionisation (EIMS) technique (Perkin-Elmer Clarus-680) and the

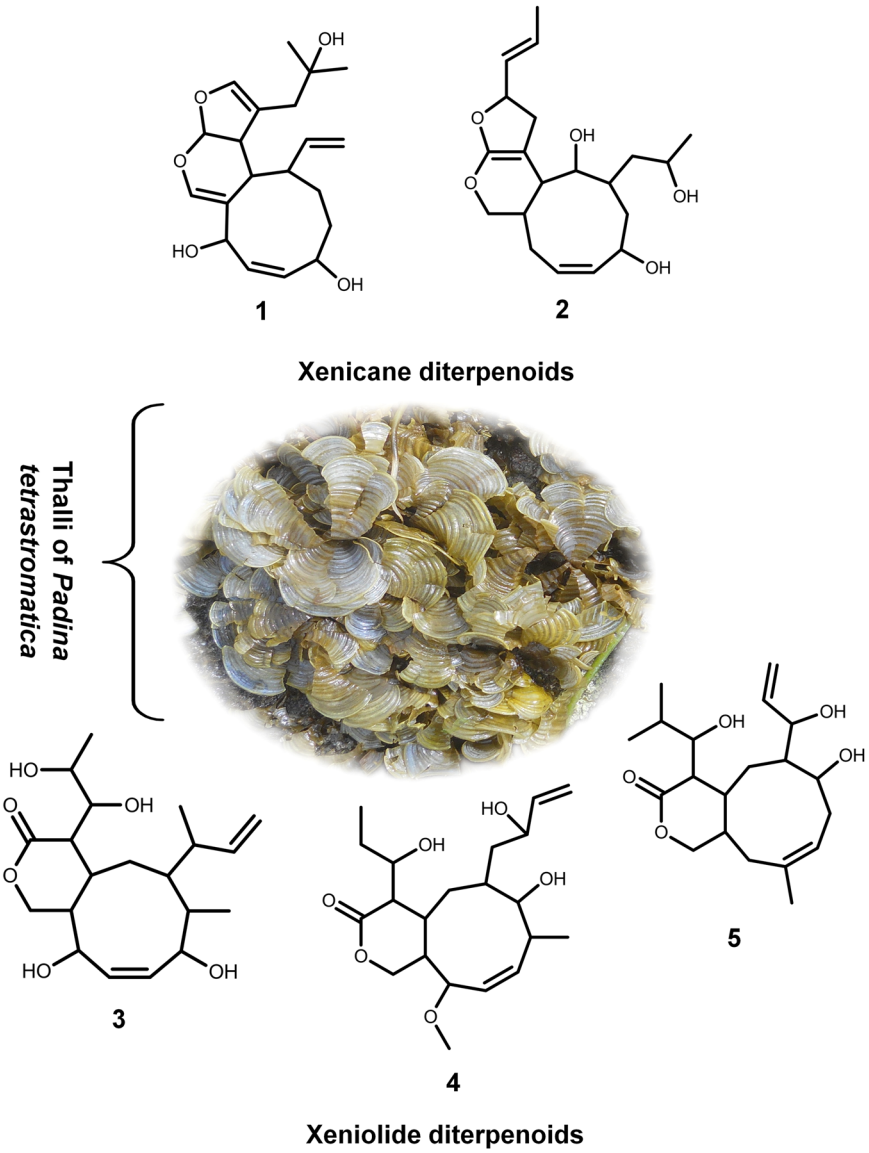

Fig. 1 Xenicane class of xenicins (**1–2**) bearing cyclonona[*d*]furo[2,3-*b*] pyrandiol and three xeniolide-type diterpenoids with octahydrocyclonona[*c*]pyran-3 (1*H*)-one backbones (**3–5**) isolated from the seaweed *Padina tetrastomatica*

fragment separation was carried out through non-polar capillary column (50 m × 0.22 mm i.d. × 0.25 µm film thicknesses). Silica gel (60–120 mesh, E-Merck, Germany; 230–400 mesh, Biotage, Sweden) was used for a range of column chromatography techniques and pre-coated plates of GF_{254} were utilized for thin layer chromatographic separation (TLC) (Chakraborty and Raola 2018).

Seaweed material and preparation of organic extracts

The seaweed used in this study was *Padina tetrastromatica* (Hauck) (family Dictyotaceae). The seaweeds were freshly collected (CMFRI voucher specimen number AB.1.1.2.1) from the south east coast of India (Gulf of Mannar between 8°48′ N, 78°9′ E and 9°14′ N, 79°14′E) by scuba diving. Seaweeds were washed with seawater to exclude the externalities followed by washing with running tap water before being shade-dried (35 ± 3 °C) for 72 h. Shade-dried samples were ground (1 kg dried), and were initially extracted with *n*-hexane {600 mL × 2, at room temperature (RT) for 24 h}, to remove pigmentous substances. The residues were extracted by reflux with solvents ethyl acetate/methanol (EtOAc/MeOH 1:1 v/v, 500 mL × 3, 60–70 °C). The crude solvent extract was collected after filtration (using Whatman No. 1 filter paper) before being evaporated (50 °C) by a rotary vacuum evaporator to one-third of the initial volume, under reduced pressure, to yield a viscous mass of crude EtOAc/MeOH extract (38 g).

Chromatographic fractionation

The EtOAc/MeOH extract (38 g) of *P. tetrastromatica* was made into a slurry with silica gel (60–120 mesh, 5 g) and

filled into a glass column (60 cm × 4 cm) loaded with adsorbent silica gel (60–120 mesh, 50 g) before being subjected to vacuum liquid chromatography. Initially, the waxy material was removed by elution with *n*-hexane. The polarity of the eluent was increased gradually by the addition of ethyl acetate (*n*-hexane:ethyl acetate 95:5–3:9, v/v) to obtain 20 column fractions (12 mL each), which were further pooled to 10 fractions (TA_{12}–TA_{22}) after TLC analysis (*n*-hexane/EtOAc, 9:1, v/v). The column fraction TA_{22} was further fractionated by flash chromatography on a silica gel column (230–400 mesh, 12 g), and elution was carried out with EtOAc/*n*-hexane (0–100%, by a step gradient mode) to yield a total of 30 column subfractions (15 mL each), which were combined to eight-column subfractions {$TA_{22(1-8)}$} after RP-C_8 HPLC {acetonitrile (CH_3CN)/H_2O, 85:15, v/v} and TLC (ethyl acetate/*n*-hexane, 3:1, v/v). Based on analytical TLC and HPLC, the homogeneous fractions were pooled and were purified by using preparative RP-C_{18} HPLC with acetonitrile and methanol as mobile phases (MeOH/CH_3CN, 4:1, v/v) to yield the pure compounds **1** and **2** (105 and 99 mg, respectively). The concentration of solvents followed by TLC (particle size 15 mm) using 30 % EtOAc/*n*-hexane supported the purity. The fractions $TA_{22\ (1-3)}$ were further purified by preparative HPLC with acetonitrile and methanol (MeOH/CH_3CN, 2:3, v/v) to afford the pure compounds **3** through **5** (112, 122 and 103 mg, respectively).

Spectral analyses

12-Ethenyl-3a,6,9,10,11,12,12a,12b-octahydro-1-(1^2-hydroxy-1^2-methyl-propyl)-cyclonona[*d*]furo[2,3-*b*]pyran-6,10-diol (1)

Colourless oil; $[\alpha]D^{22}$ –34 (c 0.96, $CHCl_3$); UV (MeOH) λ_{max} (log ε): 249 nm (2.61); TLC (Si gel GF_{254} 15 mm; 30% EtOAc/*n*-hexane, v/v); R_f: 0.55; R_t (RP-C_8 HPLC, MeOH:CH_3CN, 4:1, v/v): 3.20 min; FTIR (ν_{max}, cm^{-1}; bending δ, stretching ν, rocking ρ): 3472 (O–H_ν, br), 1112, 1076 (C–O_ν), 2923 (C–H_ν), 1621 (C = C_ν), 1510 (C = C_ν), 1459 (C–H_δ), 1182 (C–C_ν), 987 (=C–H_δ); ^{1}H-NMR (Fig. S1, Table 1), ^{13}C-NMR (Fig. S2, Table 1), ^{1}H-^{1}H-COSY (Fig. S4) and HMBC data (Fig. S5, Table 1); EIMS *m/z* calcd. for $C_{20}H_{28}O_5$ 348.1937, found 348.1941 $[M]^+$ (Δ1.1 ppm).

1,2,5,5a,6,9,10,11,12,12a-Decahydro-11(11^2-hydroxypropyl)-2-[(*E*)-2^1-propenyl] cyclonona[*d*]-furo[2,3-*b*] pyran-9,12-diol (2)

Yellow oil; $[\alpha]D^{22}$ –37 (c 1.80, $CHCl_3$); UV (MeOH) λ_{max} (log ε): 235 (3.1), 254 (3.7) nm; TLC (Si gel GF_{254} 15 mm; 30 % EtOAc/*n*-hexane) R_f: 0.54; R_t (RP-C_8 HPLC, MeOH: CH_3CN, 4:1, v/v): 3.24 min; FTIR (ν_{max} cm^{-1}): 3452 (O–H_ν, br), 1220 (C–O_ν), 2931 (C–H_ν), 1644 (C=C_ν), 1510 (C = C_ν), 1470 (C–H_δ), 1380 (C–H_ρ), 1169 (C–C_ν), 970 (=C–H_δ), 885, 746 (C–H_δ); ^{1}H-NMR (Fig. S8, Table 1), ^{13}C-NMR (Fig. S9, Table 1), ^{1}H-^{1}H-COSY (Fig. S11) and HMBC data (Fig. S13, Table 1); EIMS *m/z* calcd. for $C_{20}H_{30}O_5$ 350.2093, found 350.2098 $[M]^+$ (Δ1.4 ppm).

4-(4^1,4^2-Dihydroxypropyl)-4,4a,5,6,7,8,11,11a-octahydro-8,11-dihydroxy-7-methyl-6-(6^1-methyl-6^2-propenyl)-cyclonona[*c*]pyran-3-(1*H*)-one (3)

Pale yellow oil; $[\alpha]D^{22}$ + 40 (c 0.16, $CHCl_3$); UV (MeOH) λ_{max} (log ε): 246.0 (2.90) nm; TLC (Si gel GF_{254} 15 mm; 30 % EtOAc/*n*-hexane) R_f: 0.40; R_t (RP-C_8 HPLC, MeOH: CH_3CN, 4:1, v/v): 4.20 min; FTIR (ν_{max}, cm^{-1}): 3473 (O–H_ν, br), 3020 (C–H_ν), 1715 (C=O_ν), 1625 (C=C_ν), 1470 (C = C_ν), 1450 (C–H_δ), 1380 (C–H_ρ), 1283 (C=O_ν), 1166 (C–C_ν), 910 (=C–H_δ), 885 (C–H_δ); ^{1}H-NMR (Fig. S15, Table 2), ^{13}C-NMR (Fig. S16, Table 2), ^{1}H-^{1}H-COSY (Fig. S18) and HMBC data (Fig. S20, Table 2); EIMS *m/z* calcd. for $C_{20}H_{32}O_6$ 368.2199, found 368.2203 $[M]^+$ (Δ1.08 ppm).

4,4a,5,6,7,8,11,11a-Octahydro-7-hydroxy-6-(6^2-hydroxy-6^3-butenyl)-4-(4^1-hydroxypropyl)-11-methoxy-8-methyl-cyclonona[*c*]pyran-3-(1*H*)-one (4)

Pale yellow oil; $[\alpha]D^{22}$ + 43 (c 0.17, $CHCl_3$); UV (MeOH) λ_{max} (log ε): 209 (3.6), 249 (3.3) nm; TLC (Si gel GF_{254} 15 mm; 20 % EtOAc/*n*-hexane) R_f: 0.48; R_t (RP-C_8 HPLC, MeOH:CH_3CN, 2:3, v/v): 4.05 min; FTIR (ν_{max}, cm^{-1}): 3451 (O–H_ν, br), 2963 (C–H_ν), 1737 (C=O_ν), 1702 (C=C_ν), 1511 (C=C_ν), 1447 (C–H_δ), 1370 (C–H_ρ), 1280 (C=O_ν), 1180 (C–C_ν), 966 (=C–H_δ), 906 (C–H_δ); ^{1}H-NMR (Fig. S22, Table 2), ^{13}C-NMR (Fig. S23, Table 2), ^{1}H-^{1}H-COSY (Fig. S25) and HMBC data (Fig. S27, Table 2); EIMS *m/z* calcd. for $C_{21}H_{34}O_6$ 382.2355, found 382.2359 $[M]^+$ (Δ1.0 ppm).

4,4a,5,6,7,8,11,11a-Octahydro-1,7-dihydroxy-4-(4^1-hydroxy-4^2-methylpropyl)-6-(6^1-hydroxy-6^2-propenyl)-10-methyl-cyclonona[*c*]pyran-3(1*H*)-one (5)

Yellow oil; $[\alpha]D^{22}$ + 39 (c 0.13, $CHCl_3$); UV (MeOH) λ_{max} (log ε): 246.0 (2.90) nm; TLC (Si gel GF_{254} 15 mm; 30 % EtOAc/*n*-hexane) R_f: 0.40; R_t (RP-C_8 HPLC, MeOH:CH_3CN, 2:3, v/v): 3.23 min; FTIR (ν_{max}, cm^{-1}): 3450 (O–H_ν, br), 3020 (C–H_ν), 1715 (C=O_ν), 1614 (C=C_ν), 1625 (C=C_ν), 1470 (C–H_δ), 1380 (C–H_ρ), 1220 (C=O_ν), 1140 (C–C_ν), 955 (=C–H_δ), 885 (C–H_δ); ^{1}H-NMR (Fig. S29, Table 2), ^{13}C-NMR (Fig. S30, Table 2), ^{1}H-^{1}H-COSY (Fig. S32) and HMBC data (Fig. S33, Table 2); EIMS *m/z* calcd. for $C_{20}H_{32}O_6$ 368.2199, found 368.2204 $[M]^+$ (Δ1.3 ppm).

Table 1 NMR spectroscopic data[a] of xenicane-type diterpenes **(1–2)** isolated from brown seaweed *P. tetrastromatica*

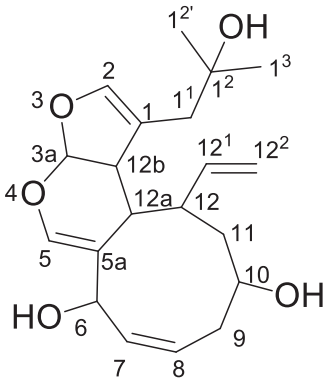

1

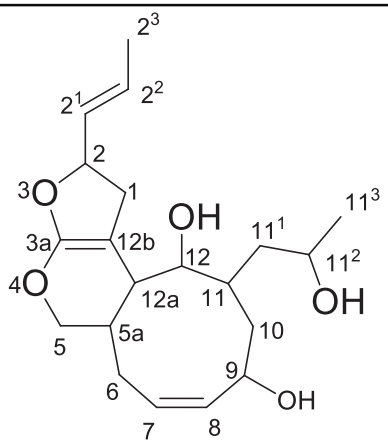

2

C. No.	^{13}C NMR	^{1}H NMR (int., mult., *J* in Hz)[b]	COSY	HMBC
1	115.25	–	–	–
1^1	39.96	2.16 (1H, *d*, *J* = 9.09 Hz) 1.91 (1H, *d*, *J* = 8.47 Hz)	–	C-1, 1^2
1^2	73.30	–	–	
$1^{2'}$	29.53	1.29 (3H, *s*)	–	C-1^3, 1^2
1^3	29.54	1.29 (3H, *s*)	–	C-1^2, 1^1
2	141.92	6.37 (1H, *s*)	–	C-1^1, 1
3	–	–	–	–
3a	104.24	6.06 (1H, *d*, *J* = 10.74 Hz)	H-12b	C-12a,5,1,2
4	–	–	–	–
5	144.10	6.41 (1H, *s*)	–	C-5a
5a	115.36	–	–	–
6	70.26	3.69 (1H, *d*, *J* = 14.70 Hz)	–	C-8, 5b
7	133.29	5.69 (1H, *m*)	H-6	C-6
8	125.48	5.51 (1H, *m*)	H-7	–
9	41.42	2.22 (1H, *m*), 1.97 (1H, *m*)	H-8	C-8
10	70.27	3.67 (1H, *m*)	H-9	C-9,8
11	38.67	1.33 (1H, *m*), 1.53 (1H, *m*)	–	C-10
12	48.95	2.03 (1H, *dd*, *J* = 12.35, 5.92)	H-11, 12^1	C-12^1, 12^2
12^1	141.08	5.72 (1H, *m*)	H-12^2	C-12^2, 11
12^2	116.46	5.00 (1H, *d*, *J* = 13.79 Hz) 4.99 (1H, *d*, *J* = 12.91 Hz)	–	–
12a	39.94	1.87 (1H, *d*, *J* = 12.62)	H-6	C-12, 5a
12b	49.82	2.17 (1H, *dd*, *J* = 10.99, 8.86 Hz)	–	C-12, 3a, 1

C. No.	^{13}C NMR	^{1}H NMR (int., mult., *J* in Hz)[b]	COSY	HMBC
1	37.74	2.68 (1H, *dd*, *J* = 8.8, 7.69 Hz), 2.30 (1H, *dd*, *J* = 13.01, 8.20 Hz)	H-2	C-12b, 3a
2	83.18	4.88 (1H, *dd*, *J* = 16.99, 8.06 Hz)	H-2^1	C-1, 2^1
2^1	129.17	5.69 (1H, *dd*, *J* = 14.47, 6.95 Hz)	H-2^2	–
2^2	130.77	5.87 (1H, *m*)	H-2^3	C-2^1, 2^3
2^3	17.65	1.82 (3H, *d*, *J* = 6.75 Hz)		–
3	–	–	–	–
3a	163.12	–	–	–
4	–	–	–	–
5	68.37	3.67 (1H, *dd*, *J* = 12.77, 7.67 Hz) 3.70 (1H, *dd*, *J* = 12.25, 7.66 Hz)	–	C-3a, 5a
5a	36.15	1.85 (1H, *m*)		C-12
6	33.72	2.01 (1H, *m*), 1.75 (H_β, *m*)	H-5a	C-7
7	132.05	5.62 (1H, *m*)	H-6	
8	132.63	5.67 (1H, *dd*, *J* = 14.47, 6.95 Hz)	–	C-7
9	72.13	4.20 (1H, *dd*, *J* = 15.60, 7.35 Hz)	H-8	C-8
10	39.54	1.29 (1H, *m*), 1.52 (H_β, *m*)	H-9	C-12, 9
11	38.69	1.22 (1H, *m*)	H-11^1	C-11^1
11^1	43.94	1.35 (1H, *t*, *J* = 5.70, 3.47 Hz)	H-11^2	–
11^2	67.75	4.07 (1H, *m*)	H-11^3	C-11^1, 11^3
11^3	23.97	1.25 (3H, *d*, *J* = 5.52 Hz)	–	–
12	71.82	3.33 (1H, *dd*, *J* = 8.76, 1.86 Hz)	H-11	
12a	41.36	1.72 (1H, *dd*, *J* = 11.46, 4.88 Hz)	H-12	C-5a, 3a, 12b
12b	94.31	–	–	–

The assignments were made with the aid of the COSY, HSQC, HMBC and NOESY experiments

[a]NMR spectra were recorded using a Bruker AVANCE III 500 MHz (AV 500) spectrometer (Bruker, Karlsruhe, Germany) in $CDCl_3$ as aprotic solvent at ambient temperature with TMS as the internal standard (δ0 ppm)

[b]Values in ppm, multiplicity and coupling constants (*J* = Hz) were indicated in parentheses. Multiplicities were allocated by ^{135}DEPT NMR spectrum

Determination of antioxidant and anti-inflammatory activities

The antioxidative activities were assessed by using DPPH (1,1-diphenyl-2-picryl hydrazyl) and $ABTS^+$ (2,2′-azino-bis-3-ethylbenzothiozoline-6-sulphonic acid diammonium salt) free radical scavenging bioassays (Wojdylo et al. 2007). In vitro anti-inflammatory activities were assessed by inhibition of pro-inflammatory cyclooxygenases-1, 2 (COX-1,2) (Larsen et al. 1996) and 5-lipoxygenase (5-LOX) (Baylac and Racine 2003) enzymes. The inhibitory activities on radicals or enzymes were plotted and recorded. The IC_{50} (concentration of samples at which it inhibits/scavenge 50 % of enzyme/radical activities) values of studied compounds and column subfractions were documented from the graph, whereas the plot of linear regression curve of percentage inhibitions against different concentrations of the compounds (or standards) were recorded as IC_{50} values

Table 2 NMR spectroscopic data[a] of xeniolide-type diterpenes **(3–5)** isolated from brown seaweed *P. tetrastromatica*

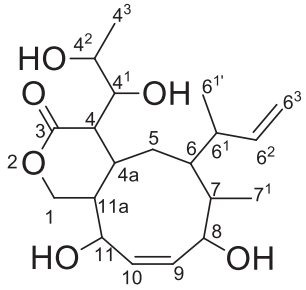

3

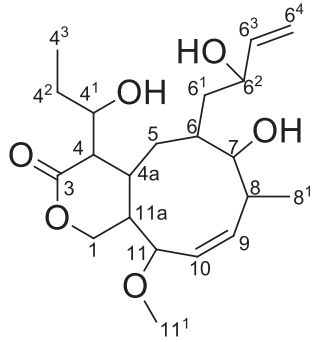

4

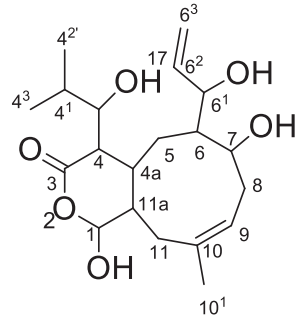

5

C. N.	^{13}C NMR	^{1}H NMR (int., mult., *J* in Hz)[b]	COSY	HMBC
1	65.75	3.95 (1H, *dd*, *J* = 10.1, 8.0 Hz) 4.22 (1H, *dd*, *J* = 9.1, 7.86 Hz)		C-3, 11a
2	–	–	–	–
3	172.35	–	–	–
4	48.80	2.21 (1H, *dd*, *J* = 9.8, 5.1 Hz)	H-4a, 4^1	C-3, 4a, 12
4a	37.55	1.62 (1H, *m*)	–	C-11a
4^1	73.49	4.03 (1H, *t*, *J* = 9.0 Hz)	H-4^2	C-3, 4, 4^2
4^2	69.36	3.42 (1H, *m*)	–	
4^3	19.32	1.21 (3H, *m*)	–	C-4^2
5	31.47	1.26 (1H, *m*), 1.01 (1H, *m*)	H-6	H-4a
6	43.98	1.15 (1H, *m*)	H-6^1	C-5
6^1	39.55	2.09 (1H, *m*)	–	C-6, 6^2
$6^{1'}$	18.34	1.22 (3H, *m*)	–	C-6^1
6^2	145.39	5.72 (1H, *m*)		C-6^3
6^3	114.82	5.01 (1H, *dd*, *J* = 19.7, 17.1 Hz), 4.99 (1H, *dd*, J = 19.7, 9.7 Hz)	–	C-6^1, $6^{1'}$

C. N.	^{13}C NMR	^{1}H NMR (int., mult., *J* in Hz)[b]	COSY	HMBC
1	65.02	3.96 (1H, *dd*, *J* = 9.7, 9.2 Hz) 4.22 (1H, *dd*, *J* = 8.20, 9.15 Hz)		C-3, 11a
2	–	–	–	–
3	172.69	–	–	–
4	50.20	2.21 (1H, *m*)	H-4^1	C-3, 4a, 4^1
4a	36.10	1.62 (1H, *m*)	–	–
4^1	69.92	4.05 (1H, *m*)	H-4^2	C-3, 4^3
4^2	27.22	1.47 (1H, *m*), 1.49 (1H, *m*)	H-4^3	C-4, 4^3
4^3	9.10	0.99 (3H, *t*, *J* = 6.4 Hz)	–	–
5	31.34	1.02 (1H, *m*) 1.26 (1H, *m*)	–	C-4a
6	40.16	1.21 (1H, *m*)	H-7, 6^1	C-5
6^1	38.63	1.42 (2H,*dd*, *J* = 6.3, 4.0 Hz)	H-6^2	C-6, 6^2
6^2	70.73	4.20 (1H, *m*)	H-6^3	–
6^3	142.32	5.92 (1H, *m*)	H-6^4	C-6^4
6^4	116.40	5.17 (1H, *m*)		C-6^2

C. N.	^{13}C NMR	^{1}H NMR (int., mult., *J* in Hz)[b]	COSY	HMBC
1	96.10	6.26 (1H, *d*, *J* = 9.6 Hz)	H-11a	C-3
2	–	–	–	–
3	171.63	–		
4	52.52	2.22 (1H, *dd*, *J* = 9.6, 3.91 Hz)	–	C-3, 4^1
4a	40.28	1.62 (1H, *m*)		C-5
4^1	71.09	3.95 (1H, *d*, *J* = 10.5 Hz)	–	–
4^2	31.50	2.07 (1H, *m*)		C-4^1
$4^{2'}$	18.60	1.05 (3H, *m*)	H-4^1, 4^3	C-4^3, 4^1
4^3	18.61	1.05 (3H, *d*, *J* = 6.52 Hz)	–	C-$4^{2'}$, 4^2, 4^1
5	30.96	1.27 (1H, *m*), 1.01 (1H, *m*)	H-6	C-6
6	40.73	1.35 (1H, *m*)	H-7, 6^1	C-7
6^1	73.68	4.10 (1H, *dd*, *J* = 10.5, 6.5 Hz)	H-6^2	C-6
6^2	140.97	5.63 (1H, *m*)	H-6^3	C-6^1, 6^3
6^3	115.03	5.11 (1H, *m*), 5.13 (1H, *m*)	–	C-6^1

Table 2 (continued)

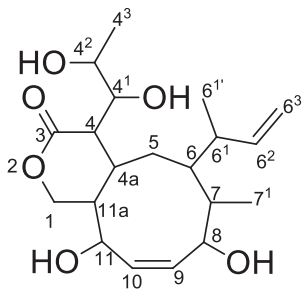

3

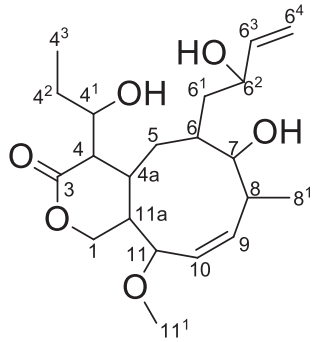

4

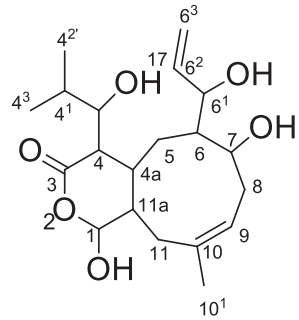

5

C. N.	^{13}C NMR	^{1}H NMR (int., mult., *J* in Hz)[b]	COSY	HMBC
7	41.86	1.45 (1H, *m*)	H-8	C-7^1
7^1	13.33	0.90 (3H, *d*, *J* = 3.2 Hz)	–	C-8
8	75.16	4.11 (1H, *t*, *J* = 9.6 Hz)	H-9	C-6
9	137.49	5.91 (1H, *d*, *J* = 11.7 Hz)	–	C-8
10	137.38	5.92 (1H, *d*, *J* = 12.7 Hz)	H-11	C-9
11	73.40	4.10 (1H, *t*, *J* = 9.5 Hz)	H-11a	C-10, 4a
11a	42.93	1.82 (1H, *m*)	–	–

C. N.	^{13}C NMR	^{1}H NMR (int., mult., *J* in Hz)[b]	COSY	HMBC
		5.20 (1H, *m*)		
7	77.02	3.35 (1H, *t*, *J* = 9.4 Hz)	–	C-6, 8^1
8	43.40	2.20 (1H, *m*)	–	C-7, 9
8^1	16.18	1.35 (3H, *d*, *J* = 6.31 Hz)	–	C-9
9	136.25	5.70 (1H, *m*)		
10	134.67	5.69 (1H, *m*)	H-11	C-9
11	82.04	3.80 (1H, *dd*, *J* = 9.1, 4.6 Hz)	H-11a	C-10, 11^1
11a	40.45	2.04 (1H, *m*)	–	–
11^1	57.17	3.30 (3H, *s*)	–	–

C. N.	^{13}C NMR	^{1}H NMR (int., mult., *J* in Hz)[b]	COSY	HMBC
7	39.10	1.53 (1H, *m*), 1.25 (1H, *m*)	–	C-8
8	66.82	4.20 (1H, *dd*, *J* = 9.1, 7.6 Hz)		
9	130.64	5.40 (1H, *dd*, *J* = 15.68 Hz)		C-8, 10
10	132.37	–		
10^1	17.73	1.73 (3H, *s*)	–	C-10, 9
11	36.76	2.02 (1H, *dd*, *J* = 11.6, 8.5 Hz) 1.76 (1H, *dd*, *J* = 12.2, 6.3 Hz)		C-10
11a	41.57	1.84 (1H, *m*)	H-4a, 11	C-11

The notations were as depicted in Table 1

(mM and/or mg mL^{-1}). The calculations of physicochemical parameters, such as molar refractivity (MR), hydrophobic descriptor (logarithm of octanol-water coefficient, log P_{ow}) and polarizability (topological polar surface area, tPSA) factors of the purified compounds by using ChemDraw Ultra 8.0 database were directed to document structure–activity relationship analyses.

In silico molecular modelling

In silico molecular modelling analysis of compounds **1**–**5** against pro-inflammatory 5-lipoxygenase was carried out using AutoDock 4 (AutoDock Tools ver. 1.5.6). These titled compounds were constructed by ACD/Chem Sketch (version 2016.2.2, Toronto, Canada) and converted as MDL-Mol files that were saved as PDB format (Open Babel). The X-ray crystal structures of pro-inflammatory 5-lipoxygenase enzyme (LOX-5) (PDB 3V99; resolution 2.25 Å) were retrieved from the Protein Data Bank (dedicated website www.pdb.org) and conformationally arranged (Swiss-Pdb Viewer, SPDBV v4.1.0). The molecular modelling analysis was carried out using Lamarckian algorithm methods, whereas the docking algorithm was run by Cygwin I–II. Following the completion of auto docking, the atomic positions RMSD (root-mean-square deviation) were examined, wherein the docking scores and binding energies were used to rank the preferred docked conformations. USCF Chimera (University of California, San Francisco, version 1.11.2) software was used to visualize the molecular docking analyses.

Statistical analysis

The assessment of significant differences between means was carried out by Statistical Program for Social Sciences 13.0 (SPSS Inc., Chicago, IL, ver. 13.0) by using one-way analysis-of-variance (ANOVA). The documentation of these values was made as mean of triplicates ± standard deviation. The ANOVA analysis was also examined means of triplicate parameters for their significance, and were represented as $P < 0.05$.

Results and discussion

Chromatographic fractionation and spectrometric analyses of secondary metabolites

Chromatographic fractionation of the organic EtOAc/MeOH extract of seaweed, *P. tetrastromatica* on silica gel resulted in eleven major column fractions (PT_1–PT_{11}), whereas percentage recovery of subfractions, PT_4 (23 %) and PT_5 (28 %) were greater compared to those displayed by PT_1 and PT_6 through PT_{11} (<15 %, $P < 0.05$). These fractions exhibited greater radical scavenging activities against DPPH ($IC_{50} < 1$ mg mL^{-1}) and $ABTS^+$ (IC_{50} 0.60–1.25 mg mL^{-1}) than those displayed by other fractions ($IC_{50} > 1.30$ mg mL^{-1}). Potential anti-inflammation bioactivities towards COX-2 and 5-LOX displayed the significance of the column subfractions, PT_4 and PT_5 ($IC_{50} <$ 0.70 mg mL^{-1}) for further chromatographic sub-fractionation, whereas the inhibiting activities of the column fractions PT_1 and PT_6–PT_{11} were significantly lesser ($IC_{50} > 1.5$ mg mL^{-1}, $P < 0.05$). Consequently, repetitive chromatographic fractionation of PT_4 and PT_5 yielded two previously unreported xenicin class of diterpenoids with 2-oxabicyclo [7.4.0]tridecane ring system (**1**–**2**) along with three xeniolide-type diterpenoids (**3–5**) with unprecedented δ-lactone cyclononane skeleton bearing an oxabicyclo[7.4.0] tridecane framework. The structural characterizations of the studied compounds were carried out by extensive spectroscopic experiments.

Spectroscopic characterization of xenicane diterpenoids isolated from *P. tetrastromatica*

The crude extract of the dried thalli of *P. tetrastromatica* was subjected to repeated chromatographic fractionation over silica gel adsorbent to acquire five xenicane classes of diterpenoid compounds (**1–5**), which were characterized by their spectroscopic data along with previous reports of literature.

12-Ethenyl-3a,6,9,10,11,12,12a,12b-octahydro-1-(1^2-hydroxy-1^2-methyl-propyl)-cyclonona[*d*]furo[2,3-*b*]pyran-6,10-diol (1)

Repeated chromatographic fractionation of *P. tetrastromatica* yielded compound **1** as a colourless oily substance. The molecular ion peak of **1** appeared at *m/z* 348, while the molecular formula $C_{20}H_{28}O_5$, implying seven unsaturation degrees, was associated with four olefinic bonds and three ring systems. The ^{13}C-NMR and $DEPT_{135}$ experiments attributed the presence of 20 carbon signals, which included the presence of two methyls (δ_C29.53, 29.54), three sp^3 methylenes (δ_C38.67, 41.42, 39.96), one sp^2 methylene (δ_C116.46), six sp^3 methines (δ_C104.24, 49.82, 39.94, 48.95, 70.27, 70.26) and four sp^2 methines (δ_C144.10, 133.29, 125.48, 141.92), along with one sp^3 (δ_C73.30) and two sp^2 (δ_C115.36, 115.25) quaternary carbons. The FTIR spectrum of **1** displayed absorption bands at 3472 cm^{-1} (–OH), 890 cm^{-1} (=CH_2) and 1112/1076 cm^{-1} (–C–O–C), which were corroborated by ^{13}C-NMR resonances at δ_C70.26, 70.27, 73.30, 29.53, 29.54 and 104.24. The lack of carbonyl absorption bands in the FTIR and the absence of signals above δ_C150 in the ^{13}C spectrum of **1** appropriately attributed that all the oxygen functionalities within the system might be in the form of ether or hydroxyl

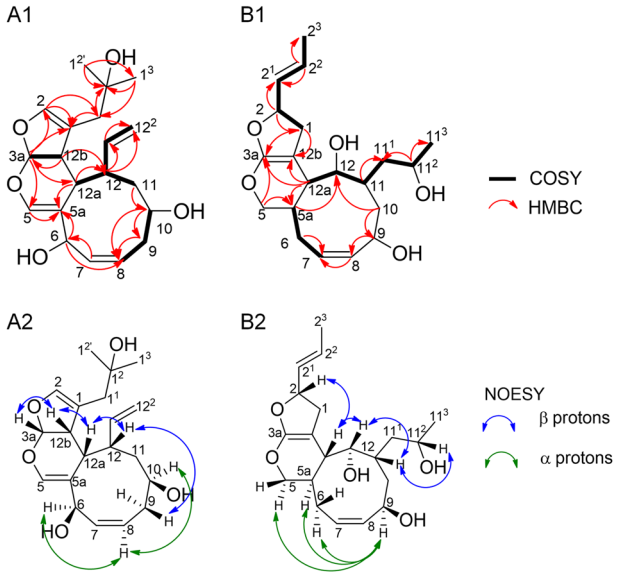

Fig. 2 Prominent **a1** ^{1}H-^{1}H COSY, selected HMBC and **a2** NOE correlations of **1**; **b1** ^{1}H-^{1}H COSY, selected HMBC and **b2** NOE correlations of **2**. The key ^{1}H-^{1}H COSY couplings were represented in bold face bonds. The key HMBC couplings have been represented by double barbed arrows. The NOESY relations were represented by double-tailed arrows, wherein the green and blue coloured arrows indicated the α- and β-protons, respectively

groups, which were also corroborated by an earlier report of the literature (Bishara et al. 2006). The ^{13}C/^{1}H-NMR experiments indicated the presence of the vinylic group due to the signals associated with δ_C141.08/δ_H5.72 (*m*) along with δ_C116.46/δ_H5.00, 4.99, which found resemblance with the values of the exocyclic double bond of the novaxenicin framework (Bishara et al. 2006). The presence of each of the two tri-substituted double bonds (δ_C115.36 and 115.25) and oxymethine (–O–CH<) groups (δ_C141.92, 144.10 and δ_H6.37, 6.41), along with one each of dioxymethine (–O–CH–O–) (δ_C104.24/δ_H6.06) and tert-alcohol functionality (δ_C73.30) attributed the presence of the novaxenicin framework (Bishara et al. 2006). Carbon signals at δ_C144.10, 141.92, 104.24, 70.27, 70.26 and 73.30 supported the presence of oxygen functionalities, and these might be due to the presence of oxymethine (–O–CH =, –O–CH<) or hydroxyl groups in **1**. The interchangeable hydroxyl protons at 70.27 (δ_H3.67), 70.26 (δ_H3.69) and 73.30 were ceased to exist upon interchange of D_2O, asserting the existence of hydroxyl groups in its vicinity. The COSYs between the protons δ_H6.06/2.17 in **1** along with HMBCs at δ_H/δ_C6.41/115.36; 1.87/115.36; 2.17/104.24; 6.06/39.94 and 6.06/144.10 proposed a six-membered ring system in **1** (Fig. 2), which was identified as a dihydro-2*H*-pyran ring system. Similarly, COSYs between the protons at δ_H1.87/2.03/1.33 and 3.67/2.22/5.51 along with HMBCs δ_H/δ_C1.87/48.95, 1.33/70.27, 3.67/41.42/125.48, 2.22/125.48, 5.69/70.26, 3.69/125.48, 3.69/115.36 and 1.87/115.36 proposed a closed loop of a nine-membered ring in **1** (Fig. 2). Thus, the positions of carbons in dihydro-2*H*-pyran with cyclononane systems were assigned from C-5 to C-5a continuously, on the basis of earlier literature (Ioannou et al. 2009; Bishara et al. 2006). The signals at C-12a (δ_C39.94) and C-5a (δ_C70.26) were identified as ring junctions based on earlier reports (Bishara et al. 2006). The COSYs of protons δ_H6.06/2.17, including HMBCs at δ_H/δ_C6.06/141.92, 6.06/115.25, 6.37/141.92 and 2.16/115.25 proposed a five-membered ring in **1** (Fig. 2), designated as dihydrofuran. Deshielded signals at δ_C104.24, 141.92 and 115.25 assigned the presence of oxymethine (–O–CH<, –O–CH=) and alkenic functionalities in **1** as the part of the dihydrofuran skeleton. Thus, the positions of carbons in dihydrofuran were disposed as C-3a, 12b, 1 and 2 based on spectroscopic assignments and previous reports of literature (Bishara et al. 2006). The carbons C-3a and C-12b were common to both dihydro-2*H*-pyran and dihydrofuran systems. Three cyclic systems, dihydrofuran, dihydro-2*H*-pyran and cyclononane in the tricyclic system were designated as **A**, **B** and **C**, respectively. Hence **A**–**B**–**C** tricyclic ring system was found to possess three spin systems, designated as **I**–**III** (H-3a/H-12b; H-12a/12/11, H-12/12^{1}/12^{2}; H-10/9/8) (depicted as bold in Fig. 2). The moiety **I** included a carbinolic proton (δ_H4.96, δ_C70.26) connected with two double-bond methines, which was coupled with a relatively deshielded methylene at δ_H2.22 and 1.97, which in turn were coupled with a sequence of protons due to carbinolic (δ_H5.51, δ_C125.48), methylene (δ_H1.33, 1.53), allylic methine (δ_H2.03), one double-bond methine (δ_H5.72) and double-bond methylene (δ_H5.00) groups. A series of $^{1,3}J_{H\text{-}C}$ correlations by HMBC were found to assemble the fragments, and to draw the planer structure of **1**.

The COSYs between δ_H6.06/2.17 (H-3a/H-12b) along with HMBCs from δ_H6.06 (H-3a) to δ_C144.10 (C-5), δ_C39.94 (C-12a), δ_C115.25 (C-1) and δ_C141.92 (C-2) and methine proton H-12b linked (δ_H2.17) to δ_C104.24 (C-3a) and δ_C48.95 (C-12) portrayed the spin systems of **I** and **II**. The HMBCs from oxymethine protons of dihydrofuran H-2 (δ_H6.37) to C-5 (δ_C115.25) and C-1^{1} (δ_C39.96) allocated the occurrence of side chain 2-methylpropan-2-ol. The methylene protons H-1^{1} (δ_H2.16/1.91), methyl protons H-1$^{2'}$ (δ_H1.29) and H-1^{3} (δ_H1.29) were associated with 2-methylpropan-2-ol displaying correlations to C-1 (δ_C115.25), C-1^{2} (δ_C73.30), C-1^{3} (δ_C29.54) and C-1^{1} (δ_C39.96). With the aid of these HMBCs, the occurrence of the **A** ring was assigned, and among them, carbons C-3a and 12b were involved in cyclic system **B**. Two terminal methyls at C-1^{2} resonating at δ_H1.29 (C-1$^{2'}$) and δ_H1.29 (C-1^{3}) were *geminal* and were assigned by HMBCs of δ_H1.29/δ_C29.53 (H-1$^{2'}$/C-1^{3}) and δ_H1.29/δ_C73.30 (H-1$^{2'}$/H-1^{2}) and between δ_H1.29/δ_C 73.30 (H-1^{3}/C-1^{2}). This spectral information was in good agreement with that of an earlier report (Bishara et al. 2006). The presence of COSYs between H-12a/H-12 (δ_H1.87/δ_H2.03), H-12/H-11 (δ_H2.03/δ_H1.33), H-12/H-9 (δ_H2.03/δ_H2.22) and H-12^{1}/H-12^{2}

(δ_H5.72/δ_H5.00) depicted the presence of second spin **II**, which displayed HMBCs between the spins **II** and **III**. The connection of spin unit **II** and ring **B** was made by HMBCs between H-12b (δ_H2.17)/C-6 (δ_C48.95) and H-12a (δ_H1.87)/C-12 (δ_C48.95), which constituted the part of cyclononane ring **C**. The correlation of exocyclic alkene to ring **C** was attributed by HMBCs between δ_H2.01/δ_C141.10 (H-12/C-12^1), δ_H5.72/δ_C116.46 (H-12^1/C-12^2), δ_H5.72/δ_C38.67 (H-12^1/C-11) and δ_H2.03/δ_C116.46 (H-12/C-12^2). The COSYs of δ_H3.67/2.22 (H-10/H-9) and δ_H2.22/5.51 (H-9/H-8) suggested the third spin system **III**. The presence of olefinic bond in the ring **C** was in accordance with the terminal alkene in the previously reported xenia diterpenoids (Ioannou et al. 2009). The connection of COSY spin system **C** and ring **B** at C-12a and C-5a was allocated by strong HMBCs between the dioxymethine proton at δ_H6.41/δ_C115.36 (H-5/C-5a) and δ_H1.87/δ_C115.36 (H-12a/C-5a). These HMBCs designated the occurrence of ring **B**, among which C-12a and C-5a were also involved in ring **C**.

The COSY spectrum exhibited the occurrence of three spin systems and HMBCs linked to the three spin systems together, allowing the assignment of the planar structure. The investigations on relative stereochemistry of the xenicin derivative were explained by NOESY experiments and coupling constants. A *trans* arrangement for the H-12a, H-5a was assigned by comparison of coupling constants recorded in previous reports (Bishara et al. 2006). The proton at δ_H6.06 (H-3a) displayed NOE with protons at H-12b (δ_H2.17). Similarly, protons at H-12b (δ_H1.87), H-12a (δ_H1.87) and H-12 (δ_H2.03) (Fig. 2) exhibited NOEs with protons at H-12a (δ_H1.87), H-12 (δ_H2.03) and H-9 (δ_H2.22), which were aligned in the β-plane of compound (**1**) (Tanaka et al. 1994). The assigned stereochemistry of hydroxyl group at C-10 and C-8 was in agreement with β-oriented protons. The chiral centres, mainly those of H-3a, 12b, 12a, 10 and H-6 were attributed by NOEs between H-3a/12b (δ_H6.06/δ_H2.17), H-12b/12a (δ_H2.17/δ_H1.87), H-8/10 (δ_H5.51/δ_H 3.67) and H-8/6 (δ_H5.51/δ_H3.69). Contrary to this β-orientation, the protons at H-8/10 (δ_H5.51/δ_H3.67) and H-8/6 (δ_H5.51/δ_H3.69) were located at the α-side of the compound **1**.

1,2,5,5a,6,9,10,11,12,12a-Decahydro-11(11^2-hydroxypropyl)-2-[(*E*)-2^1-propenyl] cyclonona[*d*]-furo[2,3-*b*] pyran-9,12-diol (2)

The chromatographic separation of the solvent extract of *P. tetrastromatica* yielded **2** as a yellow oil. The molecular ion peak of **2** was appeared at *m/z* 350, while the molecular formula $C_{20}H_{30}O_5$, implying six unsaturation degrees, was associated with three olefinic bonds and three ring systems. The ^{13}C-NMR of **2** along with DEPT$_{135}$ attributed the occurrence of 20 signals of carbons, which included two methyls (δ_C17.65, 23.97), five sp^3 methylenes (δ_C68.37, 39.54, 33.72, 37.74, 43.94), seven sp^3 methines (δ_C41.36, 71.82, 38.69, 72.13, 36.15, 83.18, 67.75), four sp^2 methines (δ_C132.60, 132.05, 129.17, 130.77), along with two sp^2 (δ_C163.12, 94.31) quaternary carbons. The interchangeable hydroxyl protons at δ_C71.82 (δ_H3.33), δ_C72.13 (δ_H4.20) and δ_C67.75 (δ_H4.07) disappeared upon D_2O interchange, which ascribed the presence of hydroxyl groups in its vicinity. The HMBCs at δ_H/δ_C3.67/163.12, 1.72/163.12, 1.72/36.15 and 3.67/36.15 proposed the six-membered ring in **2** (Fig. 3), which was designated as dihydro-2*H*-pyran. The occurrence of deshielded signals at δ_C94.31, 163.12 and 68.37 suggested the existence of alkenic functionalities and oxygenated carbons in **2** as the part dihydro-2*H*-pyran in **2**. Similarly, COSYs between protons at δ_H1.72/3.33/1.22 and 5.62/2.01/1.85 along with HMBCs at δ_H/δ_C1.72/33.72, 2.01/71.82, 1.29/71.82/72.13, 4.20/132.63, 5.67/132.05 and 2.01/132.05 assigned the nine-membered ring in **2** (Fig. 3). The COSYs of protons δ_H2.68/4.88, including HMBCs at δ_H/δ_C2.68/94.31/163.12 and 4.88/37.74, reckoned the five-membered ring in **2** (Fig. 3). Deshielded signals at δ_C163.12 and 94.31 attributed the alkenic and oxygenated carbons in **2** as the part of dihydrofuran (positions were assigned as C-3, 4, 12 and 13). The COSYs between H-2/H-2^1 (δ_H4.88/5.69), H-2/H-1 (δ_H4.88/2.30) and HMBCs at H-2/C-2^1 (δ_H4.88/ δ_C129.17), H-2/C-1 (δ_H4.88/δ_C37.74) (Fig. 3) depicted the presence of dioxymethine group in **2** (Bishara et al. 2006). Particularly, compounds **1** and **2** exhibited similarities in their structures excluding the substitutions at C-2 and C-11. In **2**, a carbon side chain with modifications was attached to C-2. The location of double bond was also shifted to C-3a/C-12b in **2**, wherein the extra substitution of propan-2-ol, and the arrangement of hydroxyls were different in **2** as compared to those found in **1**, and that these attributions were confirmed by three COSY spins (**I–III**) and HMBCs. The COSY spectrum revealed the existence of three spin units (**I–III**) that were connected together by HMBCs in the tricyclic system, affirming the planer structure of **2**. The side chains prop-2-ene and propan-2-ol linked to the tricyclic ring system were supported by the spin systems **I** and **II**. The ^{1}H and ^{13}C-NMR experiments disclosed higher resemblance of **2** with **1**, in that former owned the similar tricyclic system, but varied in composition of the side chain.

Relative stereochemistries of **2** were demonstrated with NOESY interactions, wherein the correlations between δ_H4.88/1.72 (H-2/12a), δ_H1.72/3.33 (H-12a/5), δ_H3.33/1.22 (H-1/11), δ_H1.22/1.35 (H-11/11^1) and δ_H1.22/4.07 (H-11/11^2) revealed the presence of these protons on the similar face of the tricyclic system (arbitrarily assigned to β). NOEs between δ_H1.85/4.20 (H-5a/H-9), δ_H2.01/4.20 (H-6/H-9) and δ_H3.67/4.20 (H-5/H-9) assigned the protons to be oriented towards the α-plane of the tricyclic system.

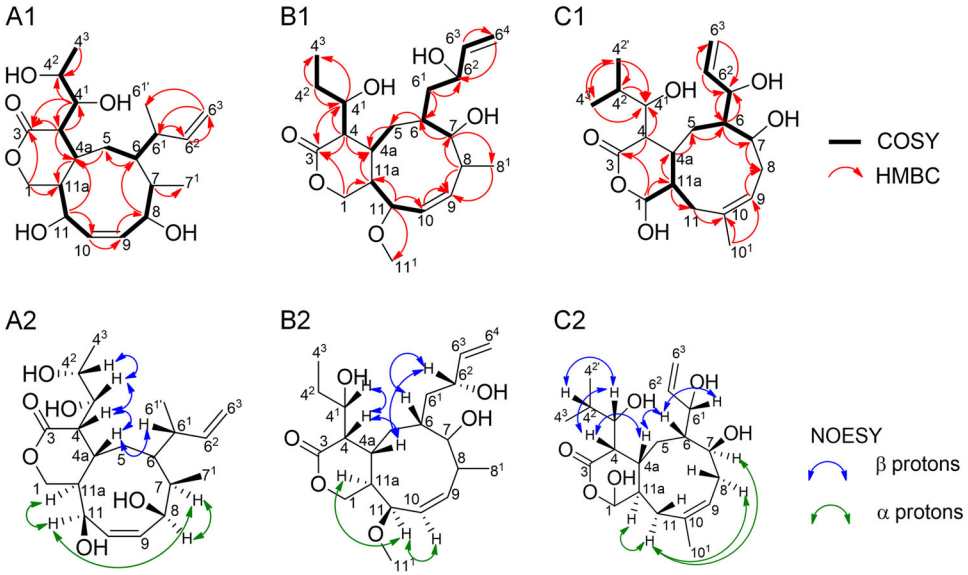

Fig. 3 Prominent **a1** ^{1}H-^{1}H COSY, selected HMBC and **a2** NOE correlations of **3**; **b1** ^{1}H-^{1}H COSY, selected HMBC and **b2** NOE correlations of **4**; **c1** ^{1}H-^{1}H COSY, selected HMBC and **c2** NOE correlations of **5**. The notations were as indicated in Fig. 2

NOESYs between H-2/H-12a, H-12a/H-12 and H-5a/H-9 established the *trans* orientation of the chiral carbons at C-12a and C-5a (Fig. 3).

4-(4^{1},4^{2}-Dihydroxypropyl)-4,4a,5,6,7,8,11,11a-octahydro-8,11-dihydroxy-7-methyl-6-(6^{1}-methyl-6^{2}-propenyl)-cyclonona[*c*]pyran-3-(1*H*)-one (3)

The chromatographic fraction of the crude extract of *P. tetrastromatica* yielded **3** as pale yellowish oil. The molecular ion peak of **3** was appeared at *m/z* 368, whereas the molecular formula $C_{20}H_{32}O_6$, implying five unsaturation degrees, was associated with three olefinic bonds and two ring systems. The spectroscopic data of **3** displayed, in conjunction with the similar substituted nine-membered cyclic system of diterpenoids **1**–**2** along with the *δ*-lactone signals at δ_C65.75 (attributed to C-1), δ_H3.95, 4.22; δ_C172.35 (C-3), δ_C48.80 (C-4); δ_H 2.21, δ_C37.55 (C-4a), δ_H1.62, and δ_C42.93 (C-11a); δ_H1.82 substituted with a 1,2-dihydroxypropyl functionality at δ_C 48.80 (C-4). The COSY spectrum revealed the existence of three spins (**I**–**III**) that were connected together by HMBCs, affirming its planer structure. An additional group of but-3-en-2-yl was observed at δ_C43.98 (C-6) associated with nine-membered cyclic ring, and the attribution was substantiated by the ^{13}C NMR bands at δ_C43.98 (C-6), δ_C39.55 (C-6^{1}), δ_C145.39 (C-6^{2}), δ_C114.82 (C-6^{3}) and δ_C18.34 (C-6$^{1'}$). These connections were supported by COSYs between δ_H1.01/1.15 (H-5/H-6), δ_H1.15/1.45 (H-6/H-7), δ_H1.15/2.09 (H-6/H-6^{1}), δ_H2.09/5.72 (H-6^{1}/H-6^{2}) and δ_H5.72/5.01 (H-6^{2}/H-6^{3}). The HMBCs between δ_H/δ_C1.15/31.47 (H-6/C-5), δ_H/δ_C2.09/43.98 (H-6^{1}/C-6), δ_H/δ_C2.09/145.39 (H-6^{1}/C-6^{2}), δ_H/δ_C1.22/39.55 (H-6$^{1'}$/C-6^{1}) and δ_H/δ_C5.01/39.55 (H-6^{3}/C-6^{1}) further substantiated the attributions.

The carbon signals of **3** showed a carbonyl carbon at δ_C172.35 (C-3) and four olefinic ^{13}C signals (one methylene, three methines), which reckoned for five degrees of unsaturation. Three COSY spin systems (**I–III**) in **3** were supported by HMBCs between the corresponding carbons and protons. The spin unit **I** was demonstrated by COSYs between δ_H1.62/2.21 (H-4a/H-4), δ_H2.21/4.03 (H-4/H-4^{1}), δ_H4.03/δ_H3.42 (H-4^{1}/H-4^{2}), which were connected to second and third spin system (**II** and **III**) by carbons C-4a and C-11a, respectively. The HMBCs at δ_H/δ_C1.01/37.55 (H-5/C-4a), δ_H/δ_C2.21/73.49 (H-4/C-4^{1}), δ_H/δ_C4.03/48.80 (H-4^{1}/C-4), δ_H/δ_C4.03/69.36 (H-4^{1}/C-4^{2}) and δ_H/δ_C1.21/69.36 (H-4^{3}/C-4^{2}) connected the different moieties in the spin system **I**. The HMBCs between δ_H/δ_C2.21/37.55 (H-4/C-4a) and δ_H/δ_C4.03/172.35 (H-4^{1}/C-3) connected the spin system to *δ*-lactone and nine-membered cyclic ring. Similarly COSY spin systems **II**, **III** and **IV** were established between the protons δ_H1.01/1.15 (H-5/H-6), δ_H1.15/2.09 (H-6/H-6^{1}); δ_H1.45/4.11 (H-7/H-8), δ_H4.11/5.91 (H-8/H-9), δ_H5.01/1.22 (H-6^{3}/H-6$^{1'}$); δ_H5.92/4.10 (H-10/H-11), δ_H4.10/1.82 (H-11/H-11a), which were connected each other by HMBCs between δ_H/δ_C4.11/43.98 (H-8/C-6), δ_H/δ_C4.10/37.55 (H-11/C-4a), δ_H/δ_C1.62/42.93 (H-4a/C-11a), δ_H/δ_C5.91/75.16 (H-9/C-8), δ_H/δ_C5.92/137.49 (H-10/C-9) and δ_H/δ_C4.10/137.38 (H-11/C-10). Relative stereochemistries of **3** were determined by NOESY experimental data, whereas the protons at δ_H 3.42 (H-4^{2}), δ_H4.03 (H-12), δ_H2.21 (H-4) and δ_H1.62 (H-4a) showed strong NOEs, such as H-4^{2}/H-4^{1}, H-4^{1}/H-4, H-4/H-4a and H-4a/H-6^{1}, respectively. These were aligned towards the *β*-face of the reference plane of **3**. On the other hand, NOEs demonstrated the spatial proximity of the H-11a (δ_H1.82) with the H-11 (δ_H4.10); H-11 (δ_H4.10) with H-7 (δ_H1.45), and H-8 (δ_H4.11) with H-7 (δ_H1.45).

These were aligned in the opposite plane of β-face of the reference plane of **3** (as α-protons).

4,4a,5,6,7,8,11,11a-Octahydro-7-hydroxy-6-(6^2-hydroxy-6^3-butenyl)-4-(4^1-hydroxypropyl)-11-methoxy-8-methyl-cyclonona[*c*]pyran-3-(1*H*)-one (4)

Compound **4** was obtained as yellowish oil, whereas the molecular ion peak of **4** was appeared at *m/z* 382, and the molecular formula was determined as $C_{21}H_{34}O_6$. The spectroscopic characteristics of **4** were comparable to those of **3** with resonances exhibited by nine-membered cyclic ring bearing methoxy group at δ_C82.04 (C-11) and substituted 2-hydroxybut-3-en-1-yl side chain at δ_C40.16 (C-6). The ^{13}C-NMR and DEPT$_{135}$ spectra displayed the occurrence of 21 signals of carbons incorporating twelve methine carbons (consisting of three olefinic methine carbons), five methylene carbons (including one olefinic methylene carbon signals and oxymethylene), three methyl carbons (including one methoxy carbon signal), suggesting five degrees of unsaturation, which proposed that **4** was a hydroxyl-substituted xeniolide diterpene. The proton NMR spectrum designated the existence of oxymethylene protons at δ_H4.22, 3.96 and methoxy protons at 3.30 (H-11^1, 3H, *s*), which were attributed to the δ_C65.02 (C-1) and δ_C57.17 (C-11^1) (Table 2) of the xenicane diterpenoid skeleton (Bishara et al. 2006).

The hydroxyl groups at C-7, C-4^1 and C-6^2 were fixed by ^{13}C-NMR signals at δ_C77.02, 69.92, and 70.73, respectively. The location of hydroxyl group at the bicyclic system was designated by HMBCs between δ_H3.35/δ_C16.18 (H-7/C-8^1), δ_H3.35/ δ_C40.16 (H-7/C-6), δ_H2.20/δ_C77.02 (H-8/C-7), and also by COSYs between δ_H1.21/3.35 (H-6/H-7). The methyl group at C-8, methoxy moiety at C-11 and alkenic bond at C-9 were associated with the fourth spin system between the protons δ_H5.69/3.80 (H-10/H-11) and δ_H3.80/2.04 (H-11/H-11a), which were coupled with HMBCs between δ_H5.69/δ_C 136.25 (H-10/C-9), δ_H3.80/ δ_C134.67 (H-11/C-10), δ_H3.80/δ_C40.45 (H-11/C-11a), δ_H2.04/δ_C36.10 (H-11a/C-4a), δ_H3.96/δ_C40.45 (H-1/C-11a) and δ_H3.80/δ_C134.67 (H-11/C-10). In the spin system **I** (side chain 1-hydroxypropyl), the protons and carbons were connected by HMBCs, δ_H2.21/δ_C73.49 (H-4/C-4^1), δ_H4.05/ δ_C172.69 (H-4^1/C-3), δ_H4.05/δ_C9.10 (H-4^1/C-4^3), δ_H1.47/ δ_C69.92 (H-4^2/C-4^1), δ_H1.47/δ_C9.10 (H-4^2/C-4^3) along with COSYs δ_H2.21/4.05 (H-4/H-4^1), δ_H4.05/1.47 (H-4^1/H-4^2), δ_H1.47/0.99 (H-4^2/H-4^3 that attributed that the spin unit **I** was linked to δ-lactone as well as fourth (**IV**) and second (**II**) spin system via HMBCs between δ_H2.21/δ_C36.10 (H-4/C-4a) and δ_H2.04/δ_C 36.10 (H-11a/C-4a), respectively. Similarly, the second spin system (**II**) was explained by COSYs between δ_H1.62/1.26 (H-4a/H-5). Relative stereochemistries of **4** were resolved by NOEs, wherein proton signal showed NOEs, such as δ_H4.05/2.21 (H-4^1/H-4), δ_H1.62/2.21 (H-4/H-4a), δ_H1.62/1.21 (H-4a/H-6), and δ_H1.21/4.20 (H-6/H-6^2). These protons were arbitrarily assigned to align in the β-face of the diterpene tricyclic system. On the other hand, NOEs showed spatial proximity between protons δ_H2.04/3.80 (H-11a/H-11) and δ_H3.80/5.69 (H-11/H-10), which were attributed to be α-oriented.

4,4a,5,6,7,8,11,11a-Octahydro-1,7-dihydroxy-4-(4^1-hydroxy-4^2-methylpropyl)-6-(6^1-hydroxy-6^2-propenyl)-10-methyl-cyclonona[*c*]pyran-3(1*H*)-one (5)

The xeniolide **5** was isolated as yellow oil, and the molecular ion peak was appeared at *m/z* 368, whereas the molecular formula $C_{20}H_{32}O_6$, implying five unsaturation degrees, was associated with three olefinic bonds and two ring systems. The compound **5** possessed substitutions on identical carbons (C-4 and C-6) of nine-membered ring, but differed in the substituted side chain patterns and occurrence of methyl moieties. The spectroscopic data of **5** were comparable with those obtained for **4** and **5**. The notable differences in the ^{13}C-NMR data of **5** from those of **4** and **5** were the substitutions at the C-1, C-4, C-6, C-7 and C-10, and corresponding variations were recorded in the ^{1}H NMR spectrum.

The compound **5** possessed an ester at δ_C171.63 (C-3), methyl groups at δ_C18.60 (C-4$^{2'}$), δ_C18.61 (C-4^3) and δ_C17.73 (C-10^1), four methylene groups at δ_C 36.76 (C-11), δ_C66.82 (C-8), and δ_C115.03 (C-6^3) (including olefinic methylene), ten methines at δ_C96.10 (C-1), δ_C52.52 (C-4), δ_C40.28 (C-4a), δ_C40.73 (C-6), δ_C39.10 (C-7), δ_C130.64 (C-9), δ_C41.57 (C-11a), δ_C71.09 (C-4^1), δ_C18.60 (C-4$^{2'}$), δ_C73.68 (C-6^1) and δ_C140.97 (C-6^2) (including one oxymethine and three olefinic methines). The three COSY spin systems (**I, II** and **III**) included 1-hydroxy-2-methylpropyl, 1-hydroxyallyl, and bicyclic ring systems, respectively. The COSY spin system **I** represented correlations between the protons δ_H2.07/1.05 (H-4^2/H-4$^{2'}$), δ_H2.07/1.05 (H-4^2/H-4^3), which were connected to δ-lactone, nine-membered ring and two other COSY spin systems (**II** and **III**) via two methine carbons {δ_C52.52 (C-4), δ_C40.28 (C-4a)}, and one quaternary carbon at δ_C71.09 (C-4^1). The HMBCs between δ_H1.05/δ_C 18.61 (H-4$^{2'}$/C-4^3) and δ_H1.05/δ_C18.60 (H-4^3/C-4$^{2'}$) supported COSY spin **I**, which was linked to δ-lactone by HMBC between δ_H1.05/δ_C71.09 (H-4^3 /C-4^1), δ_H1.05/ δ_C71.09 (H-4$^{2'}$/C-4^1), δ_H2.22/δ_C171.63 (H-4/C-3) and δ_H2.22/δ_C71.09 (H-4/C-12). The HMBC at H-6/C-7 connected COSY spin system **I** to nine-membered cyclic system, and the spin system included the cross-peaks at δ_H1.01/ 1.35 (H-5/H-6), δ_H1.35/1.53 (H-6/H-7), δ_H1.35/4.10 (H-6/ H-6^1) and δ_H4.10/5.63 (H-6^1/H-6^2). Similarly, COSY spin system **III** was accompanied by protons δ_H1.76/1.84 (H-11/ H-11a), δ_H1.84/1.62 (H-11a/H-4a), δ_H1.84/6.26 (H-11a/H-

1), wherein the methyl group substituted at C-10 (δ_C132.37) was correlated to the bicyclic ring system of xeniolide **5** by HMBCs at δ_H1.73/δ_C130.64 (H-10[1]/C-9) and δ_H1.73/δ_C132.37 (H-10[1]/C-10). The NOE data established that the protons at H-4[2], H-4[1], H-4, H-4a and H-6 exhibited spatial correlations, such as H-4[2]/H-4[1], H-4[1]/H-4, H-4/H-4a, H-4a/H-6 and H-6/H-6[1], and thus, oriented in the similar reference plane of the molecule. These were arbitrarily attributed as β-aligned. Consequently, the protons at H-11a, H-11, H-8 and H-7 were aligned towards the α-face of the molecule. The protons at chiral centres C-4[1], C-4, C-4a, C-6 and C-6[1] were arranged in the β-face of the molecule, whereas those at chiral centres C-11a and C-7 were arranged towards the α-face.

Bioactive potentials of diterpenes 1-5 isolated from *P. tetrastromatica*

The organic extract of *P. tetrastromatica* derived five diterpene derivatives, which displayed potential anti-inflammatory and antioxidative activities in various in vitro systems (Table 3). Significant differences ($P < 0.05$) in radical scavenging properties were recorded amongst the xenicin (**1–2**) and α-tocopherol against $ABTS^+$ ($IC_{50} \sim 1.91$ mM; $P < 0.05$) and DPPH ($IC_{50} \sim 1.64$ mM) radicals. Significantly higher DPPH scavenging activity was observed for xeniolide **5** (IC_{50} 1.73 mM) followed by **4** and xenicins (**2**, **3**) ($IC_{50} \sim 1.92$ mM, $P < 0.05$), in declining order. In addition, the $ABTS^+$ scavenging efficacy was significantly higher for **5** and **4** ($IC_{50} \sim 2.03$ mM) as related to those revealed by the diterpene metabolites **1** through **3** (~2.30 mM, $P < 0.05$). Anti-inflammatory activities against 5-LOX and COX-2 were significantly higher for **5** (IC_{50} 1.88 and 1.41 mM, respectively) as compared to other homologues in this series ($IC_{50} < 2.26$ mM; $P < 0.05$). The compound **5** registered greater anti-5-LOX potential (IC_{50} 1.88 mM) than that exhibited by ibuprofen (IC_{50} 4.50 mM; $P < 0.05$). The greater selectivity indices of studied diterpenes (IC_{50}anti-COX-1/IC_{50}anti-COX-2>1) as compared to that displayed by ibuprofen (0.43) inferred higher anti-inflammatory selectivity against COX-2. Previous reports of literature inferred that oxidative stress directed the generation of free radicals, which in turn, caused inflammation and related pathophysiological conditions (D'Orazio et al. 2012; Joy and Chakraborty 2017a). Thus, it is fitting to state that the higher antioxidative potentials of the studied compounds could be correlated to their anti-inflammation properties. Inflammation reactions were found to be concomitant with the formation of inflammatory prostaglandins or leukotrienes by enzymes, such as cyclooxygenases and lipoxygenase. The studied compounds from *P. tetrastromatica* were found to reduce the formation of inflammatory prostaglandins because of their potential inhibition of pro-inflammatory agents.

The physicochemical parameters of the studied xenicins (**1–2**) and xeniolides (**3–5**) corroborated the structural attributions that were accountable for targeted bioactive potentials (Joy and Chakraborty 2017b). The bioactivities were essentially associated with electronic {polarizability (Pl) and topological polar surface area (tPSA)} and lipophilic parameters ($\log P_{ow}$ logarithmic value of octanol-water coefficient), and not by the steric factors. It is of note that the steric factor of **4** and **5** ($P > 820\ cm^3$) were greater than xenicane class of diterpenoids (**1–2**, $P < 780\ cm^3$) evidently due to the occurrence of the bulk bicyclic skeleton of the xeniolides (**3–5**). However, the electronic parameters were found to play illustrious role to govern the bioactive potentials (Wang et al. 2007; Chakraborty and Raola 2018). The total numbers of electron-localized centres were lesser in **1** and **2** as designated by the assessment of electronic descriptors, thus resulting in their lower polarizability, than those documented with the xeniolides (**3–5**) (Table 3). The $\log P_{ow}$ of **5** was found to be within the desirable range (~1.95), which might cause a suitable lipophilic–hydrophobic relation (Lipinski 2004) and receptor binding (Huuskonen et al. 2000; McNally et al. 2007) leading to higher target bioactivities than other studied compounds.

In silico molecular docking studies of the xenicane derivatives

The studied compounds were subjected to in silico molecular docking analysis against pro-inflammatory 5-lipoxygenase (LOX-5), and the results were evaluated by their RMSD data. The molecular docking parameters, such as binding energy, docking score, inhibition constant, hydrogen bonding interactions, intermolecular energy and torsional free energy between the ligands and the active sites of 5-lipoxygenase were documented in Table 4. The grid box of potential binding site was assigned as $x = 40.120$, $y = 39.326$, $z = 41.254$. Among the studied compounds, xenicanes **1** and **2**, on molecular docking analysis with 5-lipoxygenase, exhibited one hydrogen bond interaction with amino residues Arg411 and Arg438 in the enzyme active site with molecular distances of 3.011 and 2.740 Å, respectively (Fig. 4). Among the xeniolide analogues, compound **5** showed three hydrogen bonded interactions with amino acid residues, one hydrogen bonded with Lys441 (2.799 Å), and two with Gln434 (2.860 and 2.886 Å). The compound **5** exhibited greater number of hydrogen bond interactions with amino acyl residues than those recorded by **3** (2.742 Å with Gln437) and **4** (2.935 Å with Asp290) (Fig. 5). The lesser distance of 2.740 Å in ligand-protien complex of compound **2** established its closer

Table 3 In vitro bioactive potentials (antioxidant and anti-inflammatory) of compounds **1**–**5** and commercially available references along with molecular descriptors (electronic, steric and hydrophobic) of the studied compounds isolated from *P. tetrastromatica*

Compounds	Antioxidant activities (IC_{50}, mM)		Anti-inflammatory activities (Inhibitory activities against pro-inflammatory enzymes, IC_{50}, mM)			
	DPPH scavenging	ABTS scavenging	COX-1 inhibitory	COX-2 inhibitory	5-LOX inhibitory	Selectivity index
1	2.16 ± 0.03^{a}	2.41 ± 0.03^{a}	2.09 ± 0.03^{a}	1.98 ± 0.01^{a}	2.50 ± 0.01^{a}	1.05 ± 0.02^{a}
2	2.03 ± 0.02^{b}	2.23 ± 0.02^{b}	2.17 ± 0.03^{b}	1.80 ± 0.03^{a}	2.31 ± 0.02^{a}	1.20 ± 0.01^{b}
3	1.97 ± 0.02^{b}	2.26 ± 0.03^{b}	2.04 ± 0.02^{a}	1.77 ± 0.03^{a}	2.34 ± 0.02^{a}	1.15 ± 0.02^{b}
4	1.75 ± 0.03^{c}	2.04 ± 0.01^{c}	2.12 ± 0.02^{b}	1.43 ± 0.01^{b}	1.92 ± 0.03^{b}	1.48 ± 0.03^{c}
5	1.73 ± 0.03^{c}	2.01 ± 0.04^{c}	2.14 ± 0.03^{b}	1.41 ± 0.02^{b}	1.88 ± 0.02^{b}	1.52 ± 0.02^{c}
Standard	1.46 ± 0.04^{cT}	1.70 ± 0.05^{cT}	0.19 ± 0.00^{bI}	0.44 ± 0.02^{cI}	4.50 ± 0.11^{cI}	0.43 ± 0.01^{dI}

Compounds	Molecular descriptors[¥]					
	Electronic		Steric			Hydrophobic
	PI ($\times 10^{-23}$ cm^3)	tPSA	*P* (cm^3)	MV (cm^3)	MR ($cm^3\ mol^{-1}$)	Log P_{OW}
1	37.87	79.15	762.9	284.5	95.53	1.17
2	37.95	79.15	775.5	289.4	95.73	1.52
3	38.74	107.22	822.1	317.6	97.73	1.29
4	40.78	96.22	867.5	331.4	102.87	1.61
5	38.74	107.22	826.4	315.6	97.73	1.93

MV molar volume, *P* parachor, *MR* molar refractivity, *log P* logarithmic scale of the octanol-water partition coefficient, *Pl* polarizability, *tPSA* topological polar surface area

The antioxidant and anti-inflammatory activities were expressed as IC_{50} values (mM)

[a,b,c,d]Column-wise values with different superscripts of this type indicate significant difference ($P < 0.05$), which implied for the statistical evaluation of the results. Triplicate values were taken and the variance analyses (ANOVA) were carried out (using Statistical Program for Social Sciences 13.0) for means of all parameters to examine the significance level ($P < 0.05$). The results were expressed as mean ± SD ($n = 3$)

[¥]The structure–activity relationship analysis was carried out by using different molecular descriptors of the purified compounds as described in the text

[T]Superscript of this type depicts α-tocopherol

[I]Superscript of this type depicts ibuprofen

Table 4 The in silico molecular docking parameters between the ligands (compounds **1**–**5**) and the active sites of 5-lipoxygenase

[a]Ligands	[b]Binding energy (kcal mol^{-1})	[b]Docking score (kcal mol^{-1})	[b]Inhibition constant Ki (μM)	[c]Hydrogen bonding interactions	[b]Intermolecular energy (kcal mol^{-1})	[b]Torsional free energy (kcal mol^{-1})
1	−6.85	7.15	9.53	Arg411	−7.45	0.60
2	−7.39	8.44	3.83	Arg438	−8.58	1.19
3	−11.48	11.72	0.003	Gln437	−11.78	0.30
4	−8.66	9.43	0.449	Asp290	−9.71	1.19
5	−11.56	11.40	0.033	Lys441, Gln437	−11.56	0.00

[a]Molecular docking simulations were carried out using Autodock 4 software tool

[b]Values were evaluated from the calculations based on the energy minimization

[c]Hydrogen bonding interactions of ligands **1**–**5** with protein 5-lipoxygenase

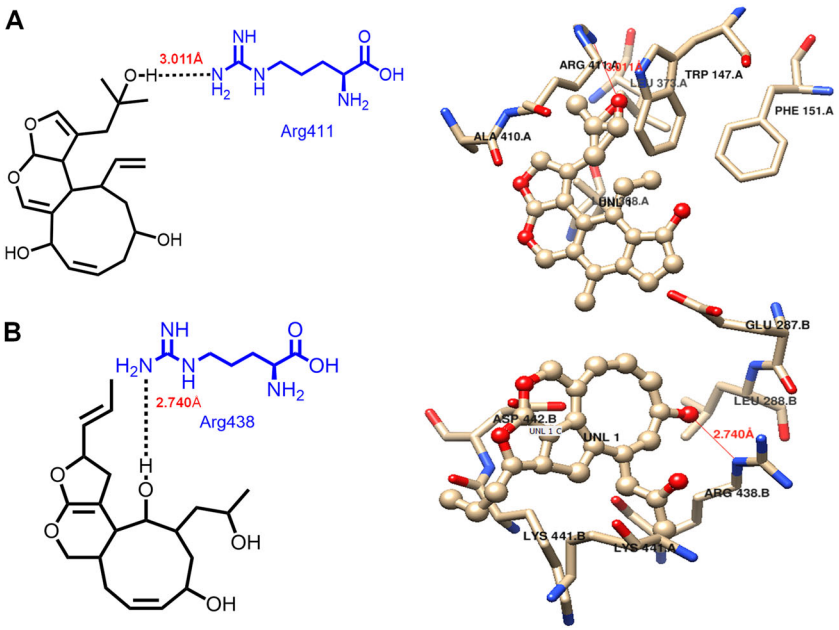

Fig. 4 Closer view of molecular binding interactions of the xenicane derivatives **1** (**a**) and **2** (**b**) in the catalytic site of protein LOX-5 as deduced from its molecular modelling simulations. The xenicanes **1** and **2** exhibited one hydrogen bond interaction with amino residues Arg411 and Arg438 in the enzyme active site with molecular distances of 3.011 and 2.740 Å, respectively

binding interaction towards protein than those displayed by xenicane **1** (3.011 Å). These results were supported by the higher in vitro anti-inflammatory activity of **2** over **1** against 5-LOX. The comparison of molecular docking parameters appropriately suggested that compound **5** exhibited close molecular interactions towards enzyme LOX-5 with least binding energy (−11.56 kcal mol^{-1}) and docking score (11.40 kcal mol^{-1}), which were corroborated with their greater potential of enzyme inhibition against LOX-5 (IC_{50} 1.88 mM) (Table 4) than those exhibited by **1**–**4**.

Conclusions

Five previously unreported xenicanes were isolated from the ethyl acetate/methanol extract of *P. tetrastromatica* by extensive chromatographic fractionation, and were characterized by detailed spectroscopic experiments. The xeniolide derivative octahydro-1,7-dihydroxy-4-(4[1]-hydroxy-4[2]-methylpropyl)-6-(6[1]-hydroxy-6[2]-propenyl)-10-methyl-cyclonona[*c*]pyran-3(1*H*)-one (**5**) showed potential antioxidant and anti-inflammatory activities, with greater selectivity index pro-inflammatory cyclooxygenase-2 than other studied xenicane derivatives and ibuprofen. Molecular docking analysis inferred that the xeniolide derivative **5** exhibited efficient interactions with 5-lipoxygenase, which validated its greater inhibitory potential against the pro-inflammatory enzyme. In particular, the xeniolide-type diterpenoids with octahydrocyclonona[*c*]pyran-3(1*H*)-one backbone could be potential functional food components for use against inflammatory diseases. The biologically active xeniolides isolated from brown seaweed *P. tetrastromatica* might constitute a promising potential natural alternative to the commercially available synthetic antioxidants and anti-inflammatory agents.

Acknowledgements The present work was supported by Science and Engineering Research Board (SERB) (grant number SR/S1/OC-96A/2012) of Department of Science and Technology, New Delhi, India. The authors thank the Director, Indian Council of Agricultural Research-Central Marine Fisheries Research Institute (ICAR-CMFRI),

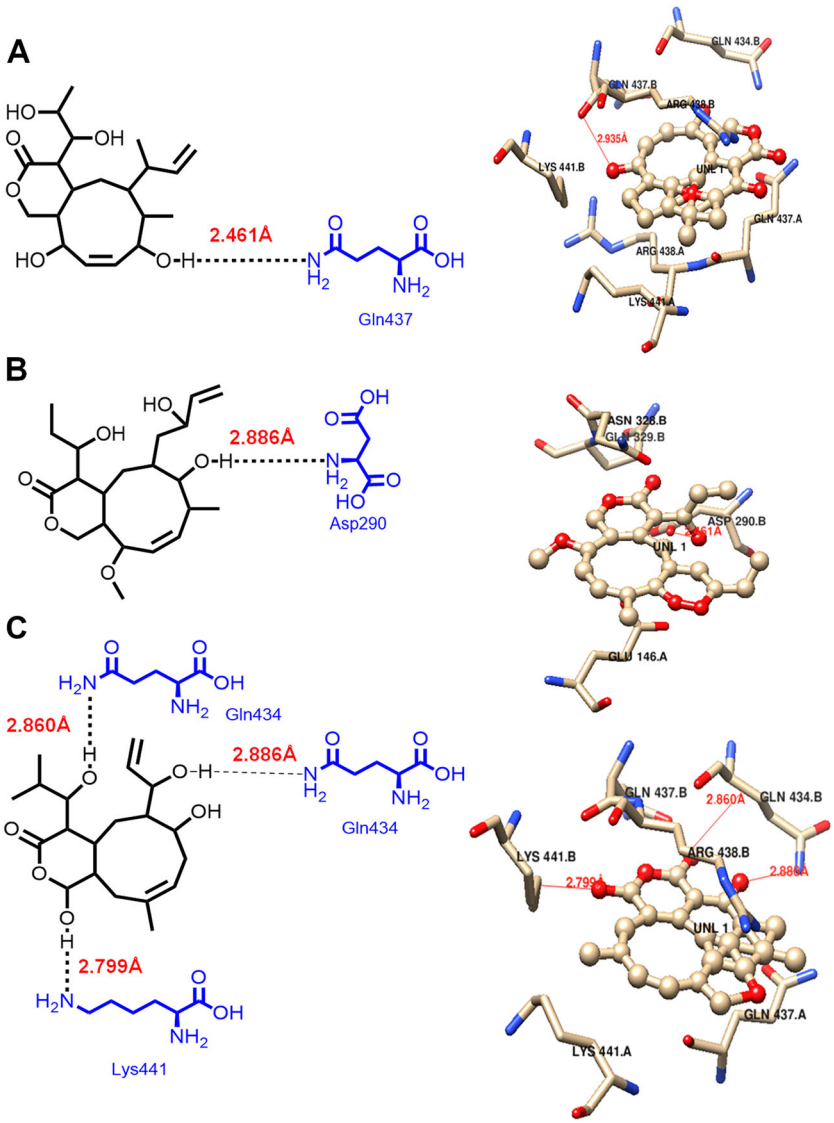

Fig. 5 Closer view of molecular binding interactions of the xeniolide derivatives **3** (**a**), **4** (**b**), and **5** (**c**) in the catalytic site of protein LOX-5 as deduced from its molecular modelling simulations. The xeniolide **5** showed three hydrogen bonded interactions with amino acid residues, one hydrogen bonded with Lys441 (2.799 Å), and two with Gln434 (2.860 and 2.886 Å). Compound **5** displayed greater number of hydrogen bond interactions with amino acyl residues than those recorded by **3** and **4**

and Head, Marine Biotechnology Division, ICAR-CMFRI for guidance and support.

Compliance with ethical standards

Conflict of interest The authors declare that they have no conflict of interest.

Ethical approval This article does not contain any studies with human participants or animals performed by any of the authors.

Publisher's note: Springer Nature remains neutral with regard to jurisdictional claims in published maps and institutional affiliations.

References

Awad NE, Selim MA, Metawe HM, Matloub AA (2008) Cytotoxic xenicane diterpenes from the brown alga *Padina pavonia* (L.). Gaill. Phytother Res 22:1610–1613

Barrento S, Camus C, Sousa-Pinto I, Buschmann AH (2016) Germplasm banking of the giant kelp: Our biological insurance in a changing environment. Algal Res 13:134–140

Baylac S, Racine P (2003) Inhibition of 5-lipoxygenase by essential oils and other natural fragment extracts. Int J Aromather 13:138–142

Bishara A, Rudi A, Goldberg I, Benayahu Y, Kashman Y (2006) Novaxenicins A–D and xeniolides I–K, seven new diterpenes from the soft coral *Xenia novaebrittanniae*. Tetrahedron 62:12092–12097

Blunt JW, Copp BR, Hu WP, Munro MHG, Northcotec PT, Prinsep MR (2009) Marine natural products. Nat Prod Rep 26(2):170–244

Chakraborty K, Raola VK (2018) Oxygenated heterocyclic metabolites with dual cyclooxygenase-2 and 5-lipoxygenase inhibitory potentials from *Rhizophora annamalayana*. Med Chem Res 27:1679–1689

Chia YY, Kanthimathi MS, Khoo KS, Rajarajeswaran J, Cheng HM, Yap WS (2015) Antioxidant and cytotoxic activities of three species of tropical seaweeds. BMC Complement Altern Med 15:339

D'Orazio N, Gammone MA, Gemello E, De Girolamo M, Cusenza S, Riccioni G (2012) Marine bioactives: Pharmacological properties

and potential applications against inflammatory diseases. Mar Drugs 10:812–833

Faulkner DJ (1998) Marine natural products. Nat Prod Rep 15:113–158

Groweiss A, Shmueli U, Kashman Y (1983) Marine toxins of *Latrunculia magnifica*. J Org Chem 48:3512–3516

Guiry MD, Nic-dhonncha E (2003) Algaebase. J Phycol 39:19–20

Huuskonen JJ, Livingstone DJ, Tetko IV (2000) Neural network modeling for estimation of partition coefficient based on atom-type electrotopological state indices. J Chem Inf Model 40:947–955

Ioannou E, Zervoub M, Ismailc A, Ktaric L, Vagiasa C, Roussisa V (2009) 2, 6-Cyclo-xenicanes from the brown algae *Dilophus fasciola* and *Dilophus spiralis*. Tetrahedron 65:10565–10572

Jimenez-Escrig A, Jimenez-Jimenez I, Pulido R, Saura-Calixto F (2001) Antioxidant activity of fresh and processed edible seaweeds. J Sci Food Agric 81:530–534

Joy M, Chakraborty K (2017a) Nutritional qualities of the low-value bivalve mollusks *Paphia malabarica* and *Villorita cyprinoides* at the estuarine waters of the southwestern coast of India. J Aquat Food Prod T 26(1):54–70

Joy M, Chakraborty K (2017b) Previously undescribed antioxidative and anti-inflammatory chromenyls bearing 3*H*-isochromenone and furanyl-2*H*-chromenyl skeletons from the venerid clam, *Paphia malabarica*. Med Chem Res 26:1708–1722

Kang SM, Lee SH, Heo SJ, Kim KN, Jeon YJ (2011) Evaluation of antioxidant properties of a new compound, pyrogallol-phloroglucinol-6, 6'-bieckol isolated from brown algae, *Ecklonia cava*. Nutr Res Pract 5:495–502

Kindleysides S, Quek SY, Miller MR (2012) Inhibition of fish oil oxidation and the radical scavenging activity of New Zealand seaweed extracts. Food Chem 133:1624–1631

Lann KL, Surget G, Couteau C, Coiffard L, Cérantola S, Gaillard F, Larnicol M, Zubia M, Guérard F, Poupart N, Valérie SP (2016) Sunscreen, antioxidant, and bactericide capacities of phlorotannins from the brown macroalga *Halidrys siliquosa*. J Appl Phycol 28:3547–3559

Larsen LN, Dahl E, Bremer J (1996) Peroxidative oxidation of leuco dichloroluorescein by prostaglandin H synthase in prostaglandin biosynthesis from polyunsaturated fatty acids. BBA 1299:47–53

Lipinski CA (2004) Lead and drug-like compounds: The rule-of-five revolution. Drug Discov Today Technol 1(4):337–341

Makkar F, Chakraborty K (2018a) Novel furanyl derivatives from the red seaweed *Gracilaria opuntia* with pharmacological activities using different in vitro models. Med Chem Res 27:1245–1259

Makkar F, Chakraborty K (2018b) Antioxidant and anti-inflammatory oxygenated meroterpenoids from the thalli of red seaweed *Kappaphycus alvarezii*. Med Chem Res 27:2016–2026

McNally VA, Rajabi M, Gbaj A, Stratford IJ, Edwards PN, Douglas KT, Bryce RA, Jaffar M, Freeman S (2007) Design, synthesis and enzymatic evaluation of 6-bridged imidazolyluracil derivatives as inhibitors of human thymidine phosphorylase. J Pharm Pharmacol 59(4):537–547

Mohsin S, Mahadevan R, Kurup GM (2014) Free-radical-scavenging activity and antioxidant effect of ascophyllan from marine brown algae *Padina tetrastromatica*. Biomed Prev Nutr 4:75–79

Plaza M, Cifuentes A, Ibanez E (2008) In the search of new functional food ingredients from algae. Trends Food Sci Technol 19(1):31–39

Tanaka J, Ogawa N, Liang J, Higa T, deNys R, Bowden BF, Carroll R, Coll J, Bernardinelli G, Jefford CW (1994) Helioxenicins A-C: Diterpenes from the blue coral *Heliopora coerulea*. Tetrahedron 50:9989–9996

Vanderah DJ, Steudler PA, Ciereszko LS, Schmitz FJ, Ekstrand JD, Van der Helm D (1977) Marine natural products. Xenicin: A diterpenoid possessing a nine-membered ring from the soft coral, *Xenia elongata*. J Am Chem Soc 99:5780–5784

Viano Y, Bonhomme D, Camps M, Briand JF, Ortalo-Magne A, Blache Y, Piovetti L, Culioli G (2009) Diterpenoids from the Mediterranean brown alga *Dictyota sp*. evaluated as antifouling substances against a marine bacterial biofilm. J Nat Prod 72:1299–1304

Wang J, Xie XQ, Hou T, Xu X (2007) Fast approaches for molecular polarizability calculations. J Phys Chem A 111:4443–4448

Wojdylo A, Oszmianski J, Czemerys R (2007) Antioxidant activity and phenolic compounds in 32 selected herbs. Food Chem 105:940–949